**Title:** Selective CDK5 Inhibition Restricts Endothelial-to-Mesenchymal Transition by Blocking a Proliferative Endothelial Fate Conversion

Dinesh Bharti[1], Tetiana Kolodiazhna[2], Sedat Kacar[1], Mathews V Varghese[1], Takanori Sano[1], Sruthi Radhakrishnan[1], Joel James[1], AJ Hinkle[1], Maki Niihori[1], Olga Rafikova[1], Alexander Statsyuk[2] and Ruslan Rafikov[1]*

Dinesh Bharti[1], Tetiana Kolodiazhna[2], Sedat Kacar[1], Mathews V Varghese[1], Takanori Sano[1], Sruthi Radhakrishnan[1], Joel James[1], AJ Hinkle[1], Maki Niihori[1], Olga Rafikova[1], Alexander Statsyuk[2] and Ruslan Rafikov[1]*

1. Department of Medicine, Division of Pulmonary, Critical Care, Sleep & Occupational Medicine, Indiana University, Indianapolis, Indiana 46202
2. College of Pharmacy, University of Houston

* To whom correspondence should be addressed:

Dr. Ruslan Rafikov rrafikov@iu.edu

**Running title:** CDK5 inhibition restricts EndMT

**Supplementary Figure 1. Molecular Docking Mapping**

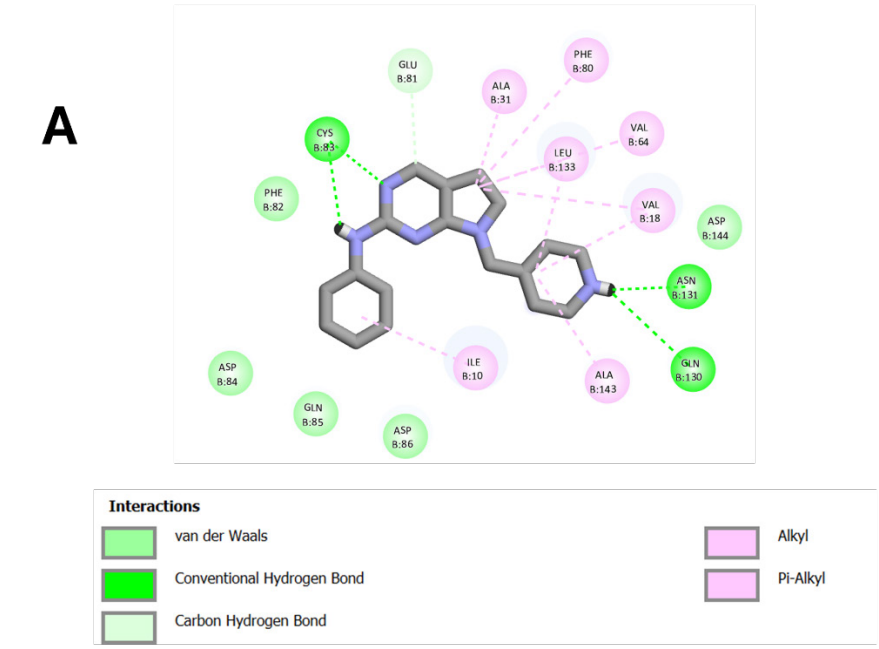


**Supplementary Figure 1. Molecular docking analysis of TK22.**

**(A)** Two-dimensional interaction map (processed by Discovery Studio) showing the predicted binding mode of TK22 within the kinase active site, highlighting key intermolecular interactions including hydrogen bonds with residues Cys 83, Asn 131, and Gln 130 of chain B, van der Waals contacts, and hydrophobic (alkyl and π-alkyl) interactions with surrounding amino acid residues.

**(B)** Three-dimensional representation of TK22 docked in the binding pocket (PDB:7VDP docked using software AutoDoc 4), illustrating the orientation of the ligand and its interactions with key residues within the active site.

**(C)** Overall docking pose of TK22 within the CDK5 kinase domain (PDB: 7VDP), showing the ligand bound in the active site pocket in the context of the full protein.

**Supplementary Figure 2. Characterization of Compound 3**

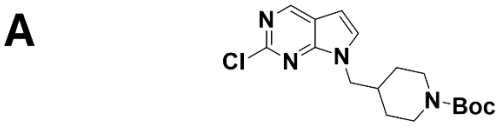


Compound 3. tert-butyl 4-[(2-chloropyrrolo[2,3]pyrimidin-7-yl)methyl]piperidine-1-carboxylate

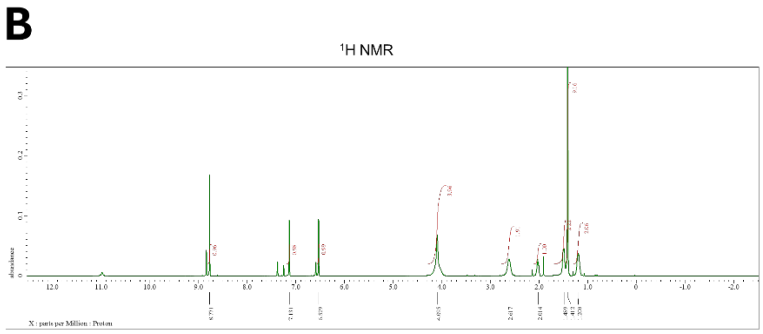


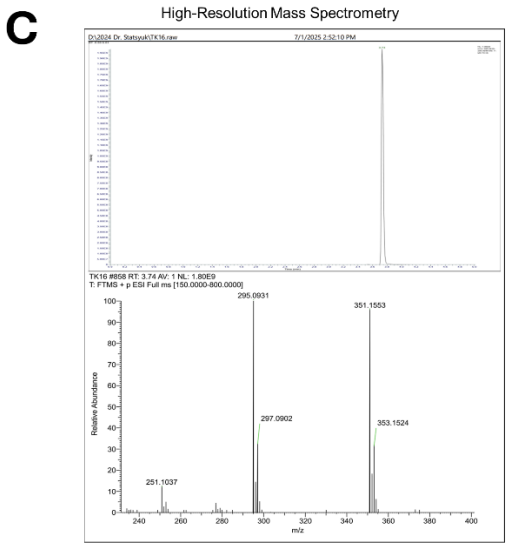


**Supplementary Figure 2. Characterization of Compound 3.**
**(A)** Chemical structure of Compound 3, tert-butyl 4-[(2-chloropyrrolo[2,3-b]pyrimidin-7-yl)methyl]piperidine-1-carboxylate.

**(B)** $^{1}$H NMR spectrum of Compound 3, confirming the proposed structure and chemical purity $^{1}$H NMR (600 MHz, Chloroform-d) δ 8.77 (s, 1H), 7.13 (d, 1H), 6.53 (d, 1H), 4.10 (s, 4H), 2.62 (s, 2H), 2.01 (m, 1H), 1.49 (t, 2H), 1.41 (s, 9H), 1.20 (t, 2H).

**(C)** High-resolution mass spectrometry (HRMS) analysis of Compound 3. The observed molecular ion peak is consistent with the calculated exact mass, confirming the molecular formula. HRMS (ESI$^{+}$): m/z calculated for $C_{17}H_{23}ClN_4O_2$ $[M+H]^{+}$: 351.15, found: 351.1553

**Supplementary Figure 3. Characterization of Compound 5**

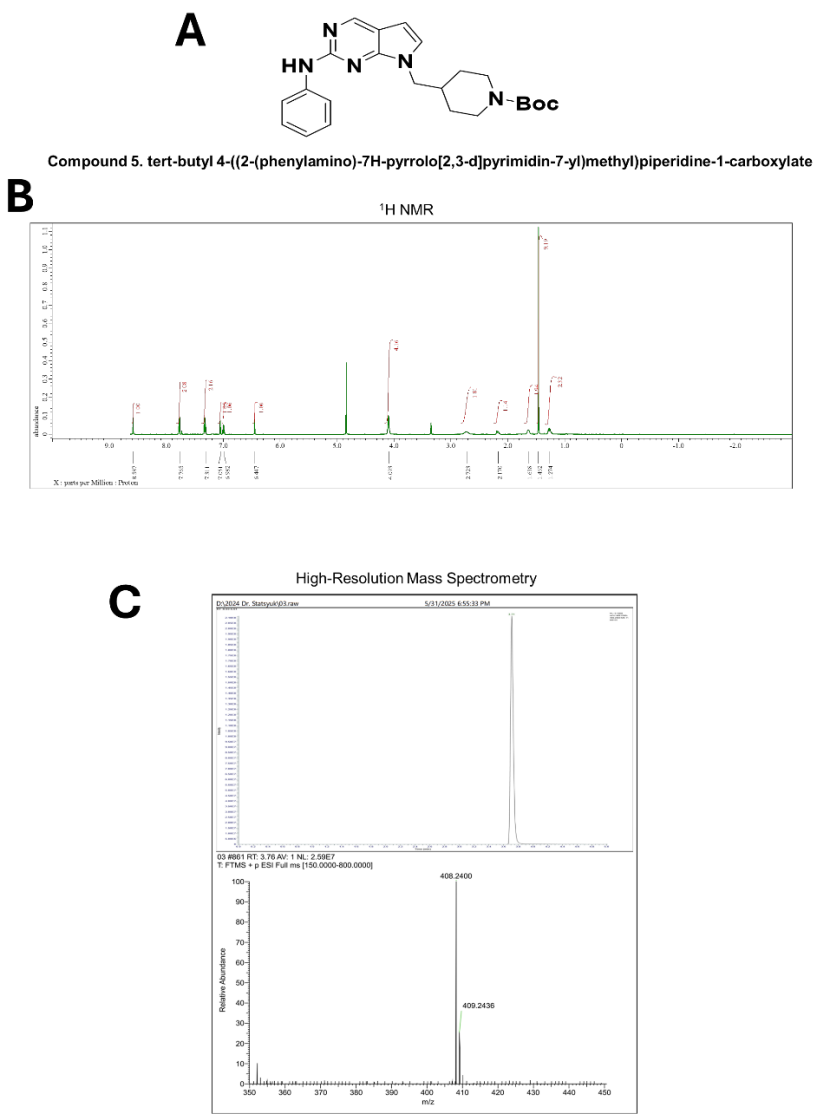


## Supplementary Figure 3. Characterization of Compound 5.

**(A)** Chemical structure of Compound 5, tert-butyl 4-[(2-(phenylamino)-7H-pyrrolo[2,3-d]pyrimidin-7-yl)methyl]piperidine-1-carboxylate.

**(B)** $^{1}$H NMR spectrum of Compound 5, confirming the proposed structure and chemical purity $^{1}$H NMR (600 MHz, Methanol-d4) δ 8.59 (s, 1H), 7.76 (d, 2H), 7.31 (t, 2H), 7.05 (d, 1H), 6.98 (t, 1H), 6.45 (d, 1H), 4.09 (d, 4H), 2.72 (s, 2H), 2.17-2.17 (m, 1H), 1.64 (d, 2H), 1.46 (s, 9H), 1.27 (q, 2H).

**(C)** High-resolution mass spectrometry (HRMS) analysis of Compound 5. The observed molecular ion peak is consistent with the calculated exact mass, confirming the molecular formula. HRMS (ESI$^{+}$): m/z calculated for $C_{23}H_{29}N_5O$ $[M+H]^{+}$: 408.24 found: 408.2400.

**Supplementary Figure 4. Characterization of TK22 1H and 13C NMR**

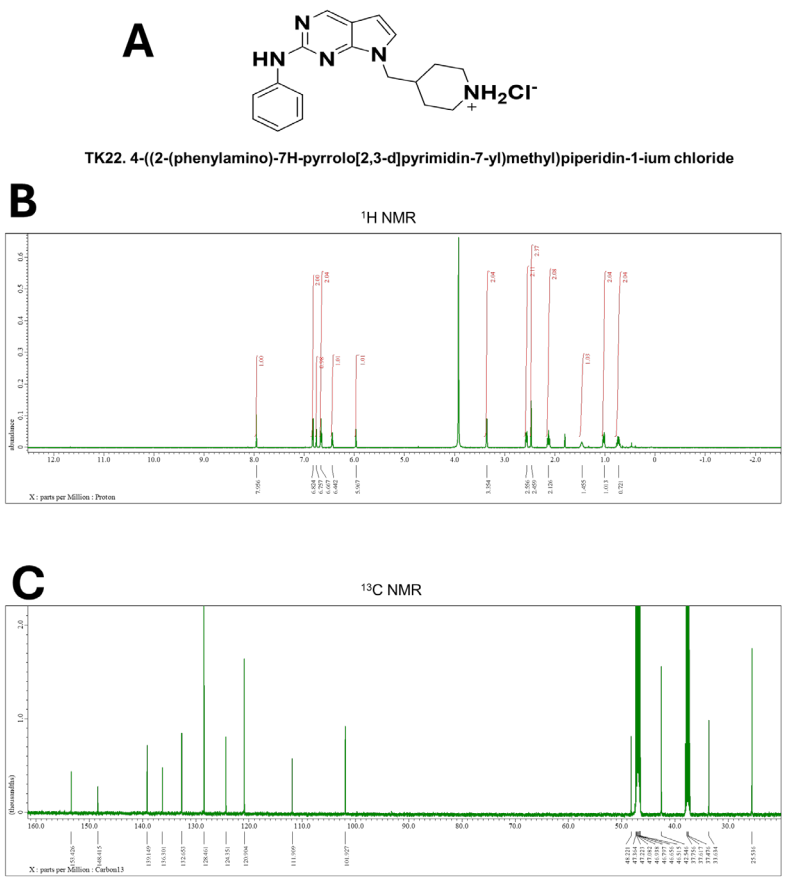


**Supplementary Figure 4. Characterization of TK22 by NMR spectroscopy.**

**(A)** Chemical structure of TK22, 4-((2-(phenylamino)-7H-pyrrolo[2,3-d]pyrimidin-7-yl)methyl)piperidin-1-ium chloride.

**(B)** $^{1}$H NMR spectrum of TK22, confirming the assigned structure and chemical purity. $^{1}$H NMR (600 MHz, dmso-d6) δ 7.96 (s, 1H), 6.82 (d, 2H), 6.76 (d, 1H), 6.67 (t, 2H), 6.44 (t, 1H), 5.97 (d, 1H), 3.35 (d, 2H), 2.56 (d, 2H), 2.46 (s, 2H), 2.13 (d, 2H), 1.46 (s, 1H), 1.01 (d, 2H), 0.72 (q, 2H).

**(C)** $^{13}$C NMR spectrum of TK22, showing carbon resonances consistent with the proposed molecular structure. $^{13}$C NMR (dmso-d6:Methanol-d4=1:5): δ 25.5 (2C, s), 33.6 (1C, s), 42.5 (2C, s), 48.2 (1C, s), 101.9 (1C, s), 111.9 (1C, s), 120.9 (2C, s), 124.3 (1C, s), 128.4 (2C, s), 132.6 (1C, s), 136.3 (1C, s), 139.1 (1C, s), 148.4 (1C, s), 153.4 C, s).

**Supplementary Figure 5. Characterization of TK22 HRMS and Purity by HPLC**

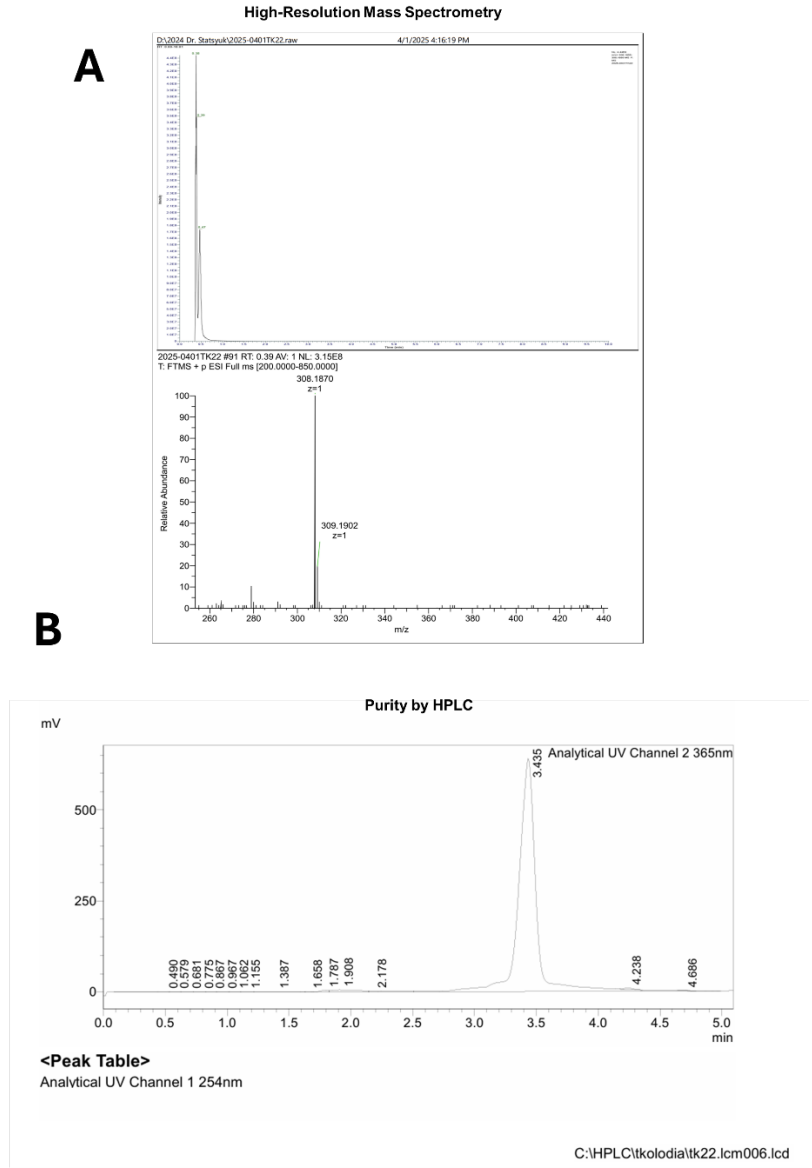


| Peak# | Ret. Time | Area | Height | Conc. | Unit | Mark | Name |
|---|---|---|---|---|---|---|---|
| 1 | 1.751 | 168379 | 26402 | 0.215 | | M | |
| 2 | 1.853 | 1256282 | 108614 | 1.602 | | | |
| 3 | 3.504 | 76106345 | 3978290 | 97.074 | | S | |
| 4 | 4.232 | 845248 | 205927 | 1.078 | | T | |
| 5 | 4.461 | 23857 | 6862 | 0.030 | | T | |
| Total | | 78400112 | 4326094 | | | | |

**Supplementary Figure 5. Characterization of TK22 by HRMS and HPLC purity analysis.**

**(A)** High-resolution mass spectrometry (HRMS) spectrum of TK22 acquired in positive ion mode, showing the observed molecular ion peak consistent with the calculated exact mass and confirming the molecular formula. HRMS ($ESI^+$): m/z calculated for $C_{18}H_{21}N_5$ $[M+H]^+$: 308.18, found: 308.1870

**(B)** Analytical HPLC chromatogram of TK22 monitored by UV detection, demonstrating high chemical purity with a single dominant peak. HPLC Ret. Time 3.5 min 97% purity.